Switching from positive to negative absorption with electromagnetically induced transparency in circuit quantum electrodynamics*

Li Hai-Chao(李海超) and Ge Guo-Qin(葛国勤)†

School of Physics, Huazhong University of Science and Technology, Wuhan 430074, *China*

(Received 17 August 2013; revised manuscript received 24 October 2013; published online 1 April 2014)

We present a theoretical study of electromagnetically induced transparency (EIT) in a superconducting quantum circuit with a tunable V-shaped energy spectrum derived from two superconducting Josephson charge qubits coupled with each other through a superconducting quantum interference device. Using the density matrix formalism and the steady-state approximation, we obtain the analytical expressions of the first-order matrix element associated with the absorption and dispersion of the probe field for two different V-type schemes. Our results show that, for this superconducting quantum system, it is possible to realize a remarkable phenomenon that dynamic conversion between EIT and EIT with amplification without population inversion. Such a unique optical feature has potential applications in quantum optical devices and quantum information processing.

Keywords: tunable V-shaped superconducting quantum circuit, electromagnetically induced transparency, amplification with and without population inversion

PACS: 42.50.Gy, 85.25.–j, 32.80.Qk **DOI:** 10.1088/1674-1056/23/5/054206

1. Introduction

Electromagnetically induced transparency (EIT)[1,2] through coherence effects has attracted a great deal of attention in recent two decades due to its wide applications in quantum optics and nonlinear optics. The essence of EIT is that an atomic coherence is induced in a multilevel system by a strong control field, which changes the response of the system to a weak probe field. Since its first experimental demonstration based on a Λ-type atomic system,[3] EIT has been investigated extensively in different atomic systems.[4–7] For example, EIT has already been demonstrated in the regime of a single ^{87}Rb atom quasi-permanently trapped inside a high-finesse optical cavity.[4] In addition, the conversion from enhanced probe transmission to enhanced probe absorption has been observed in a degenerate three-level Λ system by turning on a second control beam counter-propagating with respect to the first beam.[8] Instead of a multilevel system, EIT phenomenon using a closed degenerate two-level system has also been studied.[9]

Circuit quantum electrodynamics (QED)[10,11] based on Josephson junctions has become a new testbed for quantum optics and has reproduced many quantum optical phenomena, including single qubit lasing,[12,13] coherent population trapping,[14] the Mollow triplet,[15] Kerr and cross-Kerr nonlinearities,[16,17] and EIT.[18–20] Furthermore, circuit QED can be used to realize the ultrastrong coupling regime between a superconducting flux qubit and a coplanar waveguide[21] previously inaccessible to the conventional atomic systems and explore novel optical phenomena emerging only in this regime. As a solid-state counterpart of cavity QED, superconducting circuits offer the inherent tunability because Josephson qubits can behave as controllable quantum two-level atoms: artificial atoms. Another important advantage is that superconducting qubits in circuit QED are stationary so that the effects of Doppler broadening can be neglected and the qubit-field interaction time is long enough for most related purposes, especially the interaction in the strong coupling regime to be achieved in a relatively simple way.[22]

Recently, EIT in superconducting circuits with different three-level configurations has been researched theoretically.[23–25] However, most of those investigations focused on single superconducting qubit with two-level structure and, as a result, a resonant cavity was indispensable to obtain a three-level system. For example, in a system consisting of a superconducting Cooper-pair box (CPB) coupled to a nanomechanical resonator (NR), it needs the NR to provide additional auxiliary energy levels to the CPB to realize EIT and EIT will disappear without the NR.[23] In this paper we propose an alternative way to demonstrate EIT employing two coupled superconducting charge qubits with a tunable V-type energy spectrum. The coupled-qubit system can offer two manifest merits: the first is multiple energy levels which are crucial to on-chip realization of cavity QED; the second is the greater tunability, compared with that of single qubit, which may lead to flexible quantum optics. Previously, quantum coherent oscillations were observed by a pulse technique in two

*Project supported by the National Natural Science Foundation of China (Grant No. 11274132) and the Natural Science Foundation of Hubei Province, China.

†Corresponding author. E-mail: gqge@hust.edu.cn

© 2014 Chinese Physical Society and IOP Publishing Ltd

coupled charge qubits.[26] The tunable qubit-cavity coupling was achieved using two transmon qubits, which greatly alleviates two major challenges in experiments of circuit QED: radiative qubit decay and qubit–qubit crosstalk.[27]

Our analysis will focus on two different V-shaped structures, which depend on the energy separation of two Josephson coupling energies E_{J1} and E_{J2} of two charge qubits. When the energy spacing between the qubits' states $|eg\rangle$ and $|ge\rangle$ is very large (i.e., $E_{J1} \gg E_{J2}$), as depicted in Fig. 1(a), eigenstates of the three-level superconducting system resemble eigenstates of the two uncoupled charge qubits. When the two excited states $|ge\rangle$ and $|eg\rangle$ are degenerate (i.e., $E_{J1} = E_{J2} = E_J$), they hybridize to provide superpositions of the independent energy levels, as shown in Fig. 1(b). Our results show that it is possible to switch from EIT to EIT with amplification (EITA) by tuning the two Josephson coupling energies E_{J1} and E_{J2}, despite of the absence of population inversion.

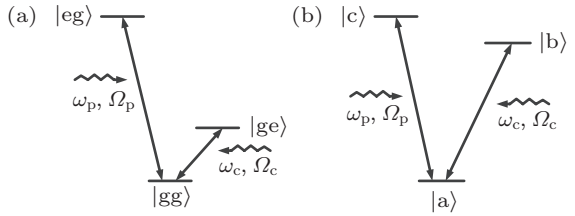


Fig. 1. Energy level diagram. (a) Schematic of the V-shaped system used to exhibit EIT for the situation when the energy spacing between the levels $|ge\rangle$ and $|eg\rangle$ is very large. (b) Schematic of the V-shaped system used to produce EITA when $|ge\rangle$ and $|eg\rangle$ are in resonance.

The remaining part of this paper is organized as follows. We first describe a theoretical model of the two-qubit system and obtain two V-shaped energy spectrums in Section 2. Using the density matrix formalism, the expressions of the first-order matrix element related to the probe transition are calculated and results are presented in Section 3. Our conclusions are given in Section 4.

2. Three-level system

The proposed V-shaped system is constructed by two independently controlled superconducting charge qubits coupled with each other through a superconducting quantum interference device (SQUID) loop, schematically presented in Fig. 2. The Hamiltonian of the coupled superconducting qubits reads

$$H_q = \sum_{i=1,2} [E_{ci}(n_i - n_{gi})^2 - E_{Ji}\cos\Theta_i] + E_m(n_1 - n_{g1}) \times (n_2 - n_{g2}) - E_{Jm}\cos(\Theta_1 - \Theta_2), \quad (1)$$

where $E_{c1,2} = 4e^2C_{\Sigma 2,1}/2(C_{\Sigma 1}C_{\Sigma 2} - C_m^2)$ are the effective Cooper-pair charging energies, $C_{\Sigma i} = C_{gi} + C_{Ji} + C_m$ for $i = 1,2$ are the sum of all capacitances connected to the corresponding island, $n_{1,2}$ are the number operators of excess Cooper-pair charges, $n_{gi} = C_{gi}V_{gi}/2e$ for $i = 1,2$ are the dimensionless gate charges and interpret the effect of the gate voltages $V_{g1,2}$, Θ_1 (Θ_2) is the phase of the first (second) superconducting island, $E_m = 4e^2C_m/(C_{\Sigma 1}C_{\Sigma 2} - C_m^2)$ is the capacitive coupling energy between the charge qubits, $E_{Ji} = E_{Ji}^{max}\cos(\pi\Phi_{xi}/\Phi_0)$ for $i = 1,2,m$ are the tunable effective Josephson coupling energies for the corresponding SQUID loop, and Φ_0 is the flux quantum.

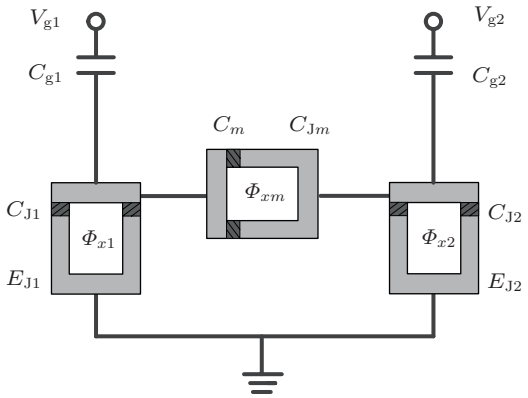


Fig. 2. Schematic of two coupled superconducting charge qubits. The two charge qubits are coupled by an SQUID loop and biased individually by an external flux $\Phi_{x1,2}$. The parameters of the two-qubit system are chosen as follows: $E_{c1}/2\pi = 220$ GHz, $E_{c2}/2\pi = 200$ GHz, $E_m/2\pi = 5$ GHz, the maximum values of the tunable Josephson coupling energies $E_{J1}^{max}/2\pi = 25$ GHz, $E_{J2}^{max}/2\pi = 20$ GHz, and $E_{Jm}^{max}/2\pi = 5$ GHz.

In the two-qubit eigenbasis $\{|ee\rangle, |eg\rangle, |ge\rangle, |gg\rangle\}$ and working at the double degeneracy point ($n_{g1} = n_{g2} = 0.5$), the Hamiltonian of the superconducting system is rewritten in spin-$\frac{1}{2}$ notation as

$$H_q = \frac{1}{2}E_{J1}\varrho_{z1} + \frac{1}{2}E_{J2}\varrho_{z2} + \frac{1}{4}E_m\varrho_{x1}\varrho_{x2} - \frac{1}{4}E_{Jm}(\varrho_{z1}\varrho_{z2} + \varrho_{y1}\varrho_{y2}). \quad (2)$$

Here we introduce a set of Pauli matrices ϱ acting on the qubit eigenstates $|e\rangle$ and $|g\rangle$. In the following calculations, by solving the eigenvalue equation of H_q under two different conditions (i.e., $E_{J1} = E_{J2}$ and $E_{J1} \gg E_{J2}$), we will obtain two different energy spectra.

Without loss of generality, we consider a special case that the two charge qubits are identical (i.e., $E_{c1} = E_{c2} = E_c$, $E_{J1} = E_{J2} = E_J$, $C_{J1} = C_{J2} = C_J$, and $C_{\Sigma 1} = C_{\Sigma 2} = C_\Sigma$). In this situation, the eigenvalues are readily written as

$$E_d = \frac{1}{4}[(E_m + E_{Jm})^2 + (E_{Jm} - 4E_J)^2]^{\frac{1}{2}}, \quad (3a)$$

$$E_c = \frac{1}{4}E_m, \quad (3b)$$

$$E_b = \frac{1}{2}E_{Jm} - \frac{1}{4}E_m, \quad (3c)$$

$$E_a = -\frac{1}{4}[(E_m + E_{Jm})^2 + (E_{Jm} - 4E_J)^2]^{\frac{1}{2}}, \quad (3d)$$

with the corresponding eigenstates being

$$|d\rangle = \sin\eta|gg\rangle + \cos\eta|ee\rangle, \quad (4a)$$

$$|\mathrm{c}\rangle = \frac{1}{\sqrt{2}}(|\mathrm{ge}\rangle + |\mathrm{eg}\rangle), \tag{4b}$$

$$|\mathrm{b}\rangle = \frac{1}{\sqrt{2}}(|\mathrm{eg}\rangle - |\mathrm{ge}\rangle), \tag{4c}$$

$$|\mathrm{a}\rangle = \sin\eta|\mathrm{ee}\rangle - \cos\eta|\mathrm{gg}\rangle, \tag{4d}$$

where $E_m \geq E_{\mathrm{J}m}$, and the parameter η satisfies the relation

$$\eta = \frac{1}{2}\arctan[(E_{\mathrm{J}m} + E_m)/(4E_{\mathrm{J}} - E_{\mathrm{J}m})]. \tag{5}$$

From the above expressions, we can see that the level spacings of the coupled-qubit system can be efficiently tuned by changing the Josephson coupling energies E_{J} and $E_{\mathrm{J}m}$. Also, it is noticeable that transitions among the four states are not arbitrary due to selection rules at the co-resonance point, as depicted in Fig. 3. The transition between the levels $|\mathrm{a}\rangle$ ($|\mathrm{b}\rangle$) and $|\mathrm{d}\rangle$ ($|\mathrm{c}\rangle$) is forbidden due to matrix elements $\langle\mathrm{a}|\boldsymbol{\varrho}_{xi}|\mathrm{d}\rangle = 0$ ($\langle\mathrm{b}|\boldsymbol{\varrho}_{xi}|\mathrm{c}\rangle = 0$) for $i = 1, 2$, while the other transitions with nonzero matrix elements are allowed. By selecting the three levels with the lowest eigenenergies (i.e., $|\mathrm{a}\rangle, |\mathrm{b}\rangle, |\mathrm{c}\rangle$), a three-level V-type system is obtained, as shown in Fig. 1(b).

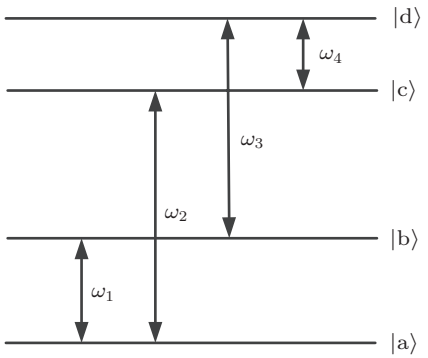


Fig. 3. Schematic of the allowed transition paths of the coupled charge qubits operated at the co-resonance point. By calculating the matrix elements of $\boldsymbol{\varrho}_{x1}$ and $\boldsymbol{\varrho}_{x2}$ between the eigenstates, it is found that there are only four possible transitions.

When the energy spacing between the levels $|\mathrm{ge}\rangle$ and $|\mathrm{eg}\rangle$ is very large (i.e., $E_{\mathrm{J}1} \gg E_{\mathrm{J}2}$), eigenstates of the coupled system resemble those of the two independent superconducting charge qubits.[27] Choosing the three levels with the lowest eigenenergies again, we obtain a second three-level V-shaped system shown in Fig. 1(a). So far, we have obtained two three-level V-type systems by using frequency selection and tuning the two Josephson coupling energies $E_{\mathrm{J}1}$ and $E_{\mathrm{J}2}$.

3. Theoretical calculation and results

In this section, adopting the density matrix formalism and the steady-state approximation, we derive the analytical expressions of the first-order matrix element associated with the absorption and dispersion of the probe field in the two V-type systems. Then, we demonstrate the switching from EIT to EITA, despite of the absence of population inversion.

Consider a closed three-level V-configuration system interacting with two semiclassical fields in Fig. 1(b). A weak probe field with Rabi frequency Ω_{p} and frequency ω_{p} couples the $|\mathrm{a}\rangle \leftrightarrow |\mathrm{c}\rangle$ transition, while a strong control field with Rabi frequency Ω_{c} and frequency ω_{c} couples the $|\mathrm{a}\rangle \leftrightarrow |\mathrm{b}\rangle$ transition. In the eigenbasis of the uncoupled qubits, the qubit-field interaction Hamiltonian is given by ($\hbar = 1$)

$$H_{\mathrm{int}} = -\frac{1}{2}(\Omega_{\mathrm{p}}\,\mathrm{e}^{-\mathrm{i}\omega_{\mathrm{p}}t}|\mathrm{e}\rangle_{11}\langle\mathrm{g}| + \Omega_{\mathrm{c}}\,\mathrm{e}^{-\mathrm{i}\omega_{\mathrm{c}}t}|\mathrm{e}\rangle_{22}\langle\mathrm{g}| + \mathrm{H.c.}), \tag{6}$$

where the Rabi frequencies of the probe and control fields are defined as $\Omega_{\mathrm{p}} = \mu_{\mathrm{ca}}E_{\mathrm{p}}$ and $\Omega_{\mathrm{c}} = \mu_{\mathrm{ba}}E_{\mathrm{c}}$ with E_{p} (E_{c}) being the amplitude of probe (control) field, μ_{ca} and μ_{ba} are the corresponding transition dipole moments. In the eigenbasis $\{|\mathrm{a}\rangle, |\mathrm{b}\rangle, |\mathrm{c}\rangle\}$ of two coupled qubits, the two flip-up operators read

$$\begin{aligned}|\mathrm{e}\rangle_{11}\langle\mathrm{g}| = &-\frac{1}{\sqrt{2}}\cos\eta|\mathrm{b}\rangle\langle\mathrm{a}| - \frac{1}{\sqrt{2}}\cos\eta|\mathrm{c}\rangle\langle\mathrm{a}| \\ &-\frac{1}{\sqrt{2}}\sin\eta|\mathrm{a}\rangle\langle\mathrm{b}| + \frac{1}{\sqrt{2}}\sin\eta|\mathrm{a}\rangle\langle\mathrm{c}|,\end{aligned} \tag{7}$$

$$\begin{aligned}|\mathrm{e}\rangle_{22}\langle\mathrm{g}| = &\frac{1}{\sqrt{2}}\cos\eta|\mathrm{b}\rangle\langle\mathrm{a}| - \frac{1}{\sqrt{2}}\cos\eta|\mathrm{c}\rangle\langle\mathrm{a}| \\ &+\frac{1}{\sqrt{2}}\sin\eta|\mathrm{a}\rangle\langle\mathrm{b}| + \frac{1}{\sqrt{2}}\sin\eta|\mathrm{a}\rangle\langle\mathrm{c}|.\end{aligned} \tag{8}$$

The total Hamiltonian of both the three-level system and two fields with frequency selection is given by

$$\begin{aligned}H_{\mathrm{V}} = &\sum_{j=\mathrm{a,b,c}} E_j|j\rangle\langle j| - \frac{1}{2\sqrt{2}}\cos\eta(\Omega_{\mathrm{c}}\,\mathrm{e}^{-\mathrm{i}\omega_{\mathrm{c}}t}|\mathrm{b}\rangle\langle\mathrm{a}| \\ &-\Omega_{\mathrm{p}}\,\mathrm{e}^{-\mathrm{i}\omega_{\mathrm{p}}t}|\mathrm{c}\rangle\langle\mathrm{a}| + \mathrm{H.c.}).\end{aligned} \tag{9}$$

It is possible to select the frequencies of the two fields so that the probe field ω_{p} and the control field ω_{c} are near resonant with the transitions $|\mathrm{a}\rangle \leftrightarrow |\mathrm{c}\rangle$ and $|\mathrm{a}\rangle \leftrightarrow |\mathrm{b}\rangle$, respectively. In this case, other transitions can be ignored in our discussion. Switching to the interaction picture, the total Hamiltonian H_{I} under the rotating-wave approximation is rewritten as

$$H_{\mathrm{I}} = \Delta|\mathrm{c}\rangle\langle\mathrm{c}| - \frac{1}{2}(\xi_{\mathrm{p}}|\mathrm{c}\rangle\langle\mathrm{a}| + \xi_{\mathrm{c}}|\mathrm{b}\rangle\langle\mathrm{a}| + \mathrm{H.c.}), \tag{10}$$

where $\xi_{\mathrm{p}} = -\frac{1}{\sqrt{2}}\Omega_{\mathrm{p}}\cos\eta$, $\xi_{\mathrm{c}} = \frac{1}{\sqrt{2}}\Omega_{\mathrm{c}}\cos\eta$, $\Delta = \omega_{\mathrm{ca}} - \omega_{\mathrm{p}}$ is the detuning of the probe field, and the control field frequency ω_{c} is assumed to match with the energy separation ω_{ba}.

The evolution of the system is governed by the equation of motion for the density matrix,

$$\frac{\mathrm{d}\rho}{\mathrm{d}t} = -\mathrm{i}[H_{\mathrm{I}}, \rho] + (\text{relaxation terms}). \tag{11}$$

According to Eqs. (10) and (11), the equations of motion for this system can be expressed as follows:

$$\dot{\rho}_{\mathrm{cc}} = -\Gamma_{\mathrm{c}}\rho_{\mathrm{cc}} + \frac{\mathrm{i}}{2}\xi_{\mathrm{p}}\rho_{ac} - \frac{\mathrm{i}}{2}\xi_{\mathrm{p}}^{*}\rho_{\mathrm{ca}}, \tag{12a}$$

$$\dot{\rho}_{\mathrm{bb}} = -\Gamma_{\mathrm{b}}\rho_{\mathrm{bb}} + \frac{\mathrm{i}}{2}\xi_{\mathrm{c}}\rho_{\mathrm{ab}} - \frac{\mathrm{i}}{2}\xi_{\mathrm{c}}^{*}\rho_{\mathrm{ba}}, \tag{12b}$$

$$\dot{\rho}_{ca} = -(\gamma_{ca} + i\Delta)\rho_{ca} + \frac{i}{2}\xi_p(\rho_{aa} - \rho_{cc}) - \frac{i}{2}\xi_c\rho_{cb}, \quad (12c)$$

$$\dot{\rho}_{ba} = -(\gamma_{ba} + i\Delta)\rho_{ba} + \frac{i}{2}\xi_c(\rho_{aa} - \rho_{bb}) - \frac{i}{2}\xi_p\rho_{bc}, \quad (12d)$$

$$\dot{\rho}_{cb} = -(\gamma_{cb} + i\Delta)\rho_{cb} - \frac{i}{2}\xi_c^*\rho_{ca} + \frac{i}{2}\xi_p\rho_{ab}, \quad (12e)$$

$$1 = \rho_{aa} + \rho_{bb} + \rho_{cc}, \quad (12f)$$

where Γ_b (Γ_c) is the relaxation rate for the level $|b\rangle$ ($|c\rangle$), γ_{ca}, γ_{ba}, and γ_{cb} are the total dephasing rates of the off-diagonal terms. In the weak probe field regime, using the steady-state approximation and keeping Ω_p up to the first-order term of perturbation expansions in Eqs. (12c)–(12e), a solution for the density matrix element ρ_{ca} is obtained as

$$\rho_{ca}^{(1)} = \frac{i\Omega_p\cos\eta}{2\sqrt{2}}\left[\frac{|\Omega_c\cos\eta|^2}{8}\frac{\rho_{aa}^{(0)} - \rho_{bb}^{(0)}}{\gamma_{ba}} - (\rho_{aa}^{(0)} - \rho_{cc}^{(0)})(\gamma_{cb} + i\Delta)\right] \times \left[(\gamma_{ca} + i\Delta)(\gamma_{cb} + i\Delta) + \frac{|\Omega_c\cos\eta|^2}{8}\right]^{-1}, \quad (13)$$

where the initial population distributions for three levels are chosen to be $\rho_{cc}^{(0)} = 0$, $\rho_{bb}^{(0)} = B/(\Gamma_b + 2B)$ and $\rho_{aa}^{(0)} = (\Gamma_b + B)/(\Gamma_b + 2B)$ with $B = |\Omega_c|^2/(2\gamma_{ba})$. It is worth noting that $\rho_{ca}^{(1)}$ is connected with two-qubit parameters E_J, E_{Jm}, and E_m through the parameter η, so that the system is distinguished from conventional atomic systems. These dependencies will also change the response characteristics of the matrix element $\rho_{ca}^{(1)}$ to the probe field to some extent. The absorption of the probe field is determined by the imaginary part of the matrix element $\rho_{ca}^{(1)}$ and the dispersion is given by the real part. This will be discussed below.

Next, we start to discuss the large energy separation case for the levels $|eg\rangle$ and $|ge\rangle$, as shown in Fig. 1(a). By using the density matrix approach and steady-state analysis again, the first-order matrix element related to the probe transition is readily obtained as

$$\rho_{ca}^{(1)} = \frac{i\Omega_p}{2}\left[(\rho_{aa}^{(0)} - \rho_{cc}^{(0)})(\gamma_{cb} + i\Delta) - \frac{|\Omega_c|^2}{4}\frac{\rho_{aa}^{(0)} - \rho_{bb}^{(0)}}{\gamma_{ba}}\right] \times \left[(\gamma_{ca} + i\Delta)(\gamma_{cb} + i\Delta) + \frac{|\Omega_c|^2}{4}\right]^{-1}, \quad (14)$$

where notations $|a\rangle = |gg\rangle$, $|b\rangle = |ge\rangle$ and $|c\rangle = |eg\rangle$ just for convenience. The expression of the first-order matrix element is analogous to that of the regular V-configuration of atomic systems, so the optical behaviors of the superconducting system seem like those of the usual atomic systems.[28]

We now intend to demonstrate the conversion between EIT and EITA in the tunable V-shaped superconducting system. In the following numerical examples, the decay rates of the system and the Rabi frequencies of the control and probe fields are $\Gamma_b/2\pi = 1.5$ MHz, $\gamma_{ca}/2\pi = 1.5$ MHz, $\gamma_{cb}/2\pi = 2$ MHz, $\gamma_{ba}/2\pi = 1.5$ MHz, $\Omega_c/2\pi = 26$ MHz, and $\Omega_p/2\pi = 4$ MHz.

Figure 4 plots both the real and the imaginary parts of the matrix element $\rho_{ca}^{(1)}$ as a function of the probe field detuning Δ for two different population distributions: (a) $\rho_{bb}^{(0)} = B/(\Gamma_b + 2B)$ and $\rho_{aa}^{(0)} = (\Gamma_b + B)/(\Gamma_b + 2B)$ with $B = |\Omega_c|^2/(2\gamma_{ba})$; (b) $\rho_{cc}^{(0)} = 1$, according to Eq. (14). In Fig. 4(a), the absorption curve presents a broadly and nearly transparent window between two absorption peaks known as the Autler–Townes peaks in quantum optics and the dispersion profile shows that the index of refractive is unity in the zero probe detuning point $\Delta = 0$, which are similar to the usual EIT in atomic systems. However, the transparency window is replaced by an amplification window due to negative absorption coefficient, i.e., the probe field is amplified instead of being absorbed, as presented in Fig. 4(b). Moreover, the roles for positive and negative dispersion are switched across the range of the probe field

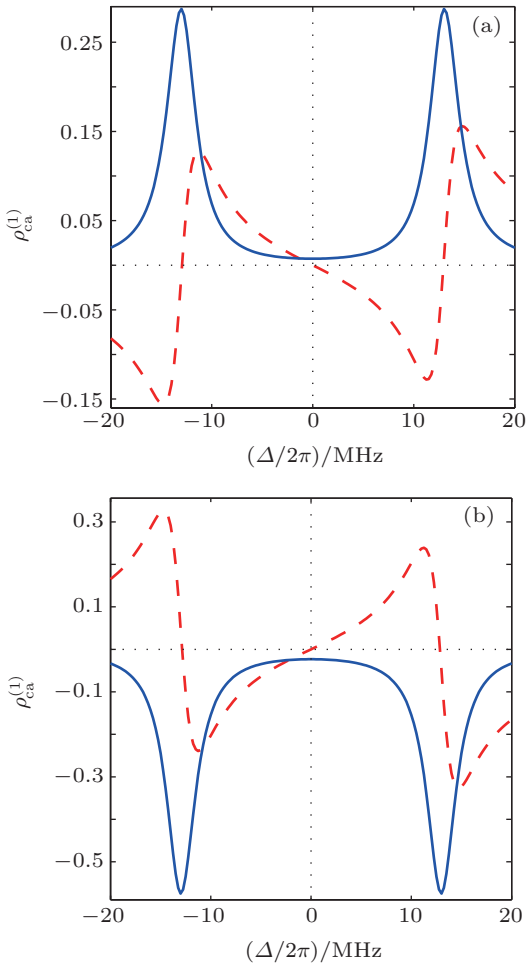


Fig. 4. (color online) Dispersion (dashed lines) and absorption (solid lines) profiles as a function of the probe field detuning Δ for two different population distributions: (a) $\rho_{aa}^{(0)} = (\Gamma_b + B)/(\Gamma_b + 2B)$ and $\rho_{bb}^{(0)} = B/(\Gamma_b + 2B)$ with $B = |\Omega_c|^2/(2\gamma_{ba})$, $\rho_{cc}^{(0)} = 0$; (b) $\rho_{aa}^{(0)} = \rho_{bb}^{(0)} = 0$, $\rho_{cc}^{(0)} = 1$.

detuning Δ, as can be seen from Figs. 4(a) and 4(b). Obviously, the phenomena of probe gain and absorption in the system result from different population distributions.

In the degenerate case of the levels $|ge\rangle$ and $|eg\rangle$, one can see that the EIT absorption and dispersion curves are similar to those in Fig. 4(b), which is better illustrated in Fig. 5, where the matrix element $\rho_{ca}^{(1)}$ is plotted for various values of the Josephson coupling energy E_J according to Eq. (13). However, this V-shaped system is in the case of without population inversion, and so we realize the inversionless amplification for the system. Figure 5 also indicates that the absorption and the width of the transparency window increase when the Josephson coupling energy E_J increases.

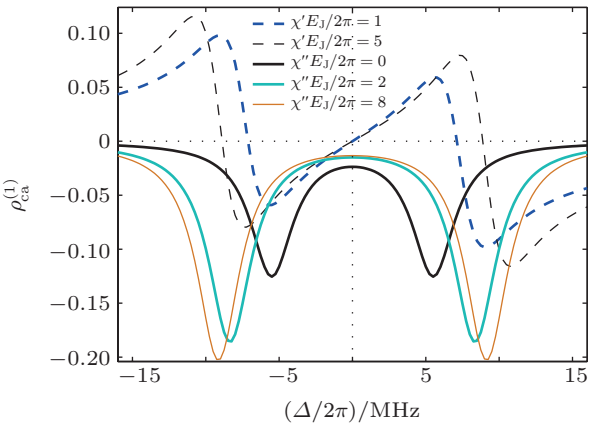


Fig. 5. (color online) Real part (dashed lines) and imaginary part (solid lines) of the matrix element $\rho_{ca}^{(1)}$ as a function of the probe field detuning Δ for different values of the Josephson coupling energy E_J (GHz). The parameters are chosen as follows: $E_m/2\pi = 5$ GHz, $E_{Jm}/2\pi = 2$ GHz.

From all the discussion above, we can know that, for the circuit QED system, through circuit design, it is possible to obtain normal optical absorption and amplification, and we can realize amplification without population inversion as well. The advantages of this system are totally shown in this configuration.

4. Conclusions

In summary, we have presented a scheme to demonstrate the switching from positive to negative absorption with EIT in a superconducting Josephson quantum system consisting of two coupled superconducting charge qubits. The analytical expressions of the steady-state matrix element related to the probe transition have been obtained via the density matrix formalism in two different V-type systems which depend on the energy separation of the two Josephson coupling energies E_{J1} and E_{J2}. When $E_{J1} \gg E_{J2}$, we observe the regular EIT phenomenon, which converts to EITA feature when $E_{J1} = E_{J2}$ despite of the absence of population inversion. This tunable optical behavior may have potential applications in quantum optical devices (such as logic gates and optical switches) and quantum coherent information storage.

References

[1] Harris S E 1997 *Phys. Today* **50** 36
[2] Fleischhauer M, Imamoglu A and Marangos J P 2005 *Rev. Mod. Phys.* **77** 633
[3] Boller K J, Imamoglu A and Harris S E 1991 *Phys. Rev. Lett.* **66** 2593
[4] Mücke M, Figueroa E, Bochmann J, Hahn C, Murr K, Ritter S, Villas-Boas C J and Rempe G 2010 *Nature* **465** 755
[5] Lazoudis A, Kirova T, Ahmed E H, Qi P, Huennekens J and Lyyra A M 2011 *Phys. Rev. A* **83** 063419
[6] Carr C, Tanasittikosol M, Sargsyan A, Sarkisyan D, Adams C S and Weatherill K J 2012 *Opt. Lett.* **37** 3858
[7] Sun Y F, Tan L and Xu Y 2013 *Chin. Phys. B* **22** 030309
[8] Chanu S R, Pandey K and Natarajan V 2012 *Europhys. Lett.* **98** 44009
[9] Dahl K, Molella L S, Rinkleff R H and Danzmann K 2008 *Opt. Lett.* **33** 983
[10] Blais A, Huang R S, Wallraff A, Girvin S M and Schoelkopf R J 2004 *Phys. Rev. A* **69** 062320
[11] You J Q and Nori F 2011 *Nature* **474** 589
[12] Astafiev O, Inomata K, Niskanen A O, Yamamoto T, Pashkin Y A, Nakamura Y and Tsai J S 2007 *Nature* **449** 588
[13] Marthaler M, Utsumi Y, Golubev D S, Shnirman A and Schön G 2011 *Phys. Rev. Lett.* **107** 093901
[14] Kelly W R, Dutton Z, Schlafer J, Mookerji B and Ohki T A 2010 *Phys. Rev. Lett.* **104** 163601
[15] Astafiev O, Zagoskin A M, Abdumalikov A A, Jr, Pashkin Y A, Yamamoto T, Inomata K, Nakamura Y and Tsai J S 2010 *Science* **327** 840
[16] Rebić S, Twanley J and Milburn G J 2009 *Phys. Rev. Lett.* **103** 150503
[17] Hu Y, Ge G Q, Chen S, Yang X F and Chen Y L 2011 *Phys. Rev. A* **84** 012329
[18] Murali K V R M, Dutton Z, Oliver W D, Crankshaw D S and Orlando T P 2004 *Phys. Rev. Lett.* **93** 087003
[19] Dutton Z, Murali K V R M, Oliver W D and Orlando T P 2006 *Phys. Rev. B* **73** 104516
[20] Zhao H, Li T F, Liu J S and Chen W 2012 *Acta Phys. Sin.* **61** 154215 (in Chinese)
[21] Niemczyk T, Deppe F, Huebl H, Menzel E P, Hocke F, Schwarz M J, Garcia-Ripoll J J, Zueco D, Hümmer T, Solano E, Marx A and Gross R 2010 *Nat. Phys.* **6** 772
[22] Clarke J and Wilhelm F K 2008 *Nature* **453** 1031
[23] Yuan X Z, Goan H S, Lin C H, Zhu K D and Jiang Y W 2008 *New J. Phys.* **10** 095016
[24] Ian H, Liu Y X and Nori F 2010 *Phys. Rev. A* **81** 063823
[25] Joo J, Bourassa J, Blais A and Sanders B C 2010 *Phys. Rev. Lett.* **105** 073601
[26] Pashkin Y A, Yamamoto T, Astafiev O, Nakamura Y, Averin D V and Tsai J S 2003 *Nature* **421** 823
[27] Srinivasan S J, Hoffman A J, Gambetta J M and Houck A A 2011 *Phys. Rev. Lett.* **106** 083601
[28] Welch G R, Padmabandu G G, Fry E S, Lukin M D, Nikonov D E, Sander F, Scully M O, Weis A and Tittel F K 1998 *Found. Phys.* **28** 621